International Journal of Engineering Trends and Technology
ISSN: 2231 – 5381 /doi:10.14445/22315381/IJETT-V69I12P227
Volume 69 Issue 12, 229-236, December, 2021

Fault Detection and Isolation Technique for Photovoltaic Based Low Voltage DC Microgrid

Prateem Pan[1], Rajib Kumar Mandal[2]

[1,2]*Department of Electrical Engineering, National Institute of Technology, Patna, Bihar, India*

[1]prateempan@gmail.com, [2]rajib@nitp.ac.in

Abstract *— This paper presents a method for the protection of a Low Voltage DC (LVDC) microgrid based on local measurements. Unlike AC microgrids, its DC counterparts encounter more protection challenges. Conventional AC protection schemes fail to address dc protection problems efficiently. This paper involves local measurement-based decisions taken by Intelligent Electronic Devices (IEDs). It initiates the trip signal based on apparent circuit resistance. Due to the absence of communication links, the method is fast and efficient for detecting and isolating faults. The simulation results show that the faulted section can be isolated within a few milliseconds. The method proves to be effective for varying fault resistance and fault location. The fault detection technique incorporates the evaluation of resistance seen by the Solid-State Circuit Breaker (SSCB) at its terminal. The efficacy of the proposed method is tested on an LVDC test system in the MATLAB/Simulink platform.*

Keywords **—** *Fault detection, Microgrid, Protection, Renewable energy sources, Short circuit faults.*

I. INTRODUCTION

documenting the recent past, a significant amount of research has been done for the integration of renewable energy sources (RES), i.e., solar photovoltaic (SPV), wind turbines, fuel cells, and battery to meet the growing electricity demand. A majority of residential and commercial loads are mainly DC loads. Due to advancements in the field of power electronic devices, it becomes easy to form a DC power grid for mitigating this load demand[1]. LVDC microgrids are widely used in telecom sectors, data centers, residential and commercial buildings. DC microgrids involve local utilization of energy. Thus the transmission and distribution losses are reduced. This results in the improvement of the overall efficiency of dc systems compared to their AC counterparts. When the majority of the loads are critical electronic components, an LVDC microgrid is the best alternative. LVDC is a potential technology for future smart distribution systems that are both cost-effective and reliable.

The DC microgrid system has more benefits in comparison to the AC system in terms of fewer power conversion stages for integrating renewable sources and simpler converter controls. DC cables are better in terms of power transfer capability as √2 times more power is transferred through DC cables than its AC counterparts[2]. However, the major challenges are in protecting the DC microgrids. In particular, the behavior of fault current in DC grids, lack of standard guidelines makes it more difficult [3]. The line impedance of the DC cable is low. This results in high fault current deviation. The rate at which fault current rises is very high in DC microgrids than in AC grids [4]. The reason behind, being the discharge of the DC link capacitor of VSC [5]. This significantly impacts the performance of power electronic switches. The existing protective devices like AC circuit breakers (ACCB) cannot be applied in DC microgrid due to the absence of natural zero crossing. So, there is a constant need for new protective devices for DC microgrid protection. In recent years Solid-State Circuit Breakers have been proposed by researchers for efficient and fast fault isolation [6].

Several protection schemes are proposed within the literature [7–14]. Most non-unit protection schemes utilize information of voltage, current, di/dt, dv/dt, and its second-order derivative for fault detection.[7]proposes an overcurrent protection scheme applied on multiterminal DC systems. The line current derivatives are employed in [8], [9], which utilizes the first and second derivatives of the current to design the protection scheme. In [10], a current derivative-based fault detection technique is used as overcurrent protection. The major drawback of this technique is that it cannot discriminate between high impedance fault and variation of load within the system. A differential current-based protection scheme is proposed in[11]. It requires a communication link to transfer data from one protection device to another for taking a decision. Thus, in the process, there is a possibility of data loss due to communication failure, affecting the performance of the protection scheme.[12]proposes a non-unit protection scheme where the AC side converters are disconnected during the faulted condition. The capacitors at the DC side supply the fault current. This leads to an overall system shutdown during the fault. Recently, signal processing techniques have been used widely in the literature. Wavelet transform and short-time Fourier transform-based techniques are proposed for fault detection in DC microgrids[13–15]. These techniques are fast and efficient enough to detect high impedance faults but misoperate during temporary and low impedance faults [16]. An LVDC microgrid protection system is proposed in this research. An LVDC microgrid is

typically connected to an ac network by bidirectional power flow converters, necessitating a separate protection mechanism. It is indeed essential to have a properly operating protection system. In DC systems, short circuit faults are the most serious problem. Most methods available in the literature involve some form of communication between the various protective equipment. This results in increased costs. Moreover, due to any communication failure, the entire protection system will fail. To address this communication failure and improve the protection and safety of small DC microgrids, i.e., residential and commercial buildings, a novel communication-less protection scheme is proposed in this work. This method is based on local measurements of voltage and currents. The gathered information is processed by the Intelligent Electronic Devices (IEDs) to make a decision for sending the tripping signal to SSCB to remove the faulty sections.

This study contributes to the development of effective fault detection and isolation method for DC microgrid protection. The fault detection technique involves evaluating the resistance seen by the SSCB at its terminals. The proposed method incorporates the decision-making based on resistance instead of voltage or current measurements directly, as seen in the case of overcurrent, overvoltage, differential, or di/dt protection schemes. Thus, the technique results in immunity to the failure of the protection system due to communication loss. Furthermore, after fault identification and isolation, the dc microgrid does not need to be completely turned down.

The paper is structured as follows: Section II discusses the DC fault analysis method. Section III discusses a resistance-based fault detection technique. In Section IV, system specifications are given. Section V explains the simulation findings in detail. Lastly, Section VI concludes the paper.

II. DC FAULT ANALYSIS

DC short circuit faults are categorized into pole - pole, and pole - ground faults. In most cases, due to insulation failure, pole to ground faults are common[17]. But pole to pole fault causes severe damage to the system, mainly the voltage source converters (VSCs). The circuit is analyzed in three different stages depicted in Fig. 1.

A. Capacitor Discharging

After the occurrence of the fault, the capacitor discharges through the DC cable impedance and fault resistance. The fault current reaches its peak value depending on various parameters like DC link capacitor voltage, DC cable impedance (π model), and fault location. The response of series RLC circuit formed is written as:

$$I(s) = \frac{\frac{V_c(0)}{L} + i_L(0)s}{s^2 + \frac{R}{L}s + \frac{1}{LC}} \quad (1)$$

Where $V_c(0)$ is the initial capacitor voltage and $i_L(0)$ is the initial inductor current. The resistance R is the summation of cable and fault resistance R_f. The fault current is expressed by

$$i(t) = \frac{V_c(0)}{L(x_2 - x_1)}[e^{-x_1 t} - e^{-x_2 t}] + \frac{i_L(0)}{(x_2 - x_1)}[-x_1 e^{-x_1 t} + x_2 e^{-x_2 t}] \quad (2)$$

The characteristic equation's roots are as follows:

$$x_{1,2} = -\frac{R}{2L} \pm \sqrt{\left(\frac{R}{2L}\right)^2 - \frac{1}{LC}} \quad (3)$$

$$x_{1,2} = -\alpha \pm \sqrt{\alpha^2 - \omega_0^2} \quad (4)$$

The current response depends upon whether $\alpha^2 < \omega_0^2$, $\alpha^2 > \omega_0^2$, or $\alpha^2 = \omega_0^2$. Based on this relationship, the response can be underdamped, overdamped, or critically damped, respectively. Taking the case of underdamped system, the current response is given by:

$$i(t) = \frac{V_c(0)}{\omega_d L} e^{-\alpha t} \sin(\omega_d t) + i_L(0) e^{-\alpha t} \left(\cos(\omega_d t) - \frac{\alpha}{\omega_d} \sin(\omega_d t) \right) \quad (5)$$

where $\omega_d = \sqrt{\omega_0^2 - \alpha^2}$

B. Diode Freewheeling

This stage is achieved after the DC link voltage of the capacitor reaches zero ($Vc=0$). This happens because of the discharge of the capacitor through the dc cable. In this entire process, commutation of the voltage source converter freewheeling diodes occurs. The cable current (natural response) is given by:

$$i_{cable} = I_0 e^{-\left(\frac{R}{L}\right)t} \quad (6)$$

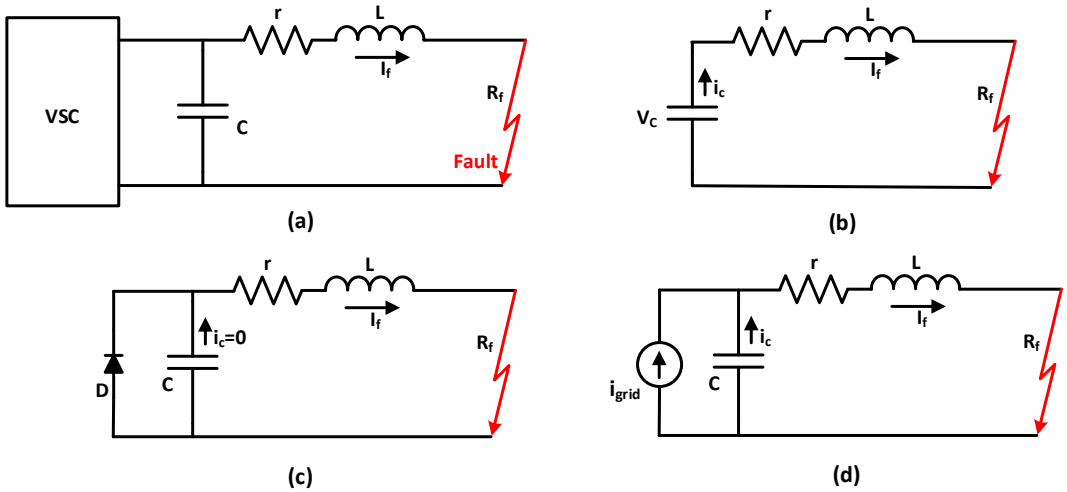

Fig. 1. (a) Fault Condition (b) Capacitor discharging (c) Diode freewheeling (d) Grid side current feeding

where I_0 is the initial value of cable current.

C. Grid Current Feeding

After the diode freewheeling, the voltage source converter acts as an uncontrolled rectifier. This results in the grid side current flowing through the fault resistance. This may damage the VSC. This is shown in Figure 1(d).

III. FAULT DETECTION TECHNIQUE

The proposed fault detection technique for the LVDC microgrid is depicted in Fig. 2. The microgrid has many sections, and each section is equipped with an IED at one end. It controls the corresponding SSCB connected in the line. The samples of voltage and the current are acquired by the IEDs. The proposed method computes the resistance seen at the terminal of that SSCB. The active resistance varies according to the distance of the fault point from the breaker[18,19].

The ratio of instantaneous voltage and current measurement is computed at the IEDs. These time-domain measurements do not require complex computational calculations. Thus, signal processing is faster and requires less memory storage. The equivalent circuit of a section of LVDC for the pole to the ground is shown in Fig. 4. The same results can be extended to large networks. The loads are divided into four zones. Each zone is equipped with an IED and SSCB to connect or isolate the circuit segment.

The dc resistive loads are represented by RL, and the cable parameters, i.e., resistance and inductance, are represented as Rc and Lc, as depicted in Fig. 2. The fault resistance is denoted by Rf. The output voltages and currents are measured at each terminal of the IEDs. For a pole-ground (PG) fault at load zone 1, the equivalent impedance in the frequency domain is given by:

$$Z_T(s) = \frac{1}{\left(\frac{1}{(R_1 + sL_1) + R_f}\right) + \sum_{j=1}^{n} Z_{Lj}} \quad (7)$$

Where $Z_{Lj}$is the impedance of the load branch. It is the summation of the equivalent resistance of the load j and cable impedance between the dc source and the load j. For the occurrence of fault F_1, as depicted in Figure 2., Z_{L1} is given as:

$$Z_{L1}(s) = R_C + sL_C + R_4 + sL_4 + R_{L1} \quad (8)$$

$$Z_{L4}(s) = R_2 + sL_2 + R_{L4} \quad (9)$$

It is assumed that the fault resistance and cable resistance are much small compared to the equivalent load resistances. So, the net equivalent impedance is given by (7). The assumptions are shown by (10)-(12).

$$\frac{1}{\left(\frac{1}{R_C + sL_C + R_f}\right)} << \frac{1}{\sum_{j=1}^{n} \frac{1}{Z_{Lj}}} \quad (10)$$

$$R_C + sL_C + R_f << \frac{1}{\sum_{j=1}^{n} \frac{1}{Z_{Lj}}} \quad (11)$$

$$Z_T(s) = R_C + sL_C + R_f \quad (12)$$

The inductive part of the impedance is neglected, as it can be noticed at only a higher frequency. Therefore, the resistance seen at the terminal is given by:

$$R_i(t) = \frac{V_i(t)}{I_i(t)} = R_C + R_f \qquad (13)$$

The fault detection technique involves the calculation of equivalent resistance on the basis of measured voltage and current samples locally at the terminals of the circuit breaker (CB). The instantaneous resistance measured is given by:

$$R_i(t) = \frac{V_i(t)}{I_i(t)} \qquad (14)$$

Where V_i and $I_i$are voltage and current samples respectively measured at the ith terminal at time instant *t*.

The calculated resistance at the terminal of SSCB, which is nearest to the faulted zone, is compared with the predefined threshold value (ε). If it is less than the threshold value ($R[i] < \varepsilon$), then a tripping signal is relayed to the breaker by the respective IED of that section to separate the faulty part. The proposed protection technique is depicted in Fig. 3. Its shows the steps required to detect the fault and send the trip signal to the circuit breaker to isolate the faulty section. Fig. 4 depicts the equivalent circuit of DG source during the faulty condition. The LVDC microgrid used in this paper has two DG sources, i.e., solar photovoltaic and battery.

IV. TEST SYSTEM

The test system used for the Low Voltage DC microgrid is modelled in the MATLAB/Simulink platform. The LVDC microgrid is considered in isolated mode and comprises two distributed generations (DGs). One being the Solar Photovoltaic and the other is the battery source.

The solar PV of 1 kW is attached by a DC-DC converter to the dc bus of 50 V. Further the LVDC network is integrated with battery and four DC resistive loads connected to the dc bus. A bidirectional DC-DC converter connects the battery to DC bus to maintain the voltage level of the bus[20], [21]. The component details and rating are given in Table 1. The IEDs and the SSCB aSre installed at the terminals of the source and the load zones connecting the DC bus[22,23]. The voltage and current sensors are used to measure the voltage and current signals at the IED terminals. These signals received at the IEDs are sampled at 4 kHz. Then after the computation of equivalent resistance at the IED terminals, trip signal is relayed to SSCB depending on the decision criteria. Thus, in case of pole-ground (PG) fault, the faulty section can be isolated from the healthy section.

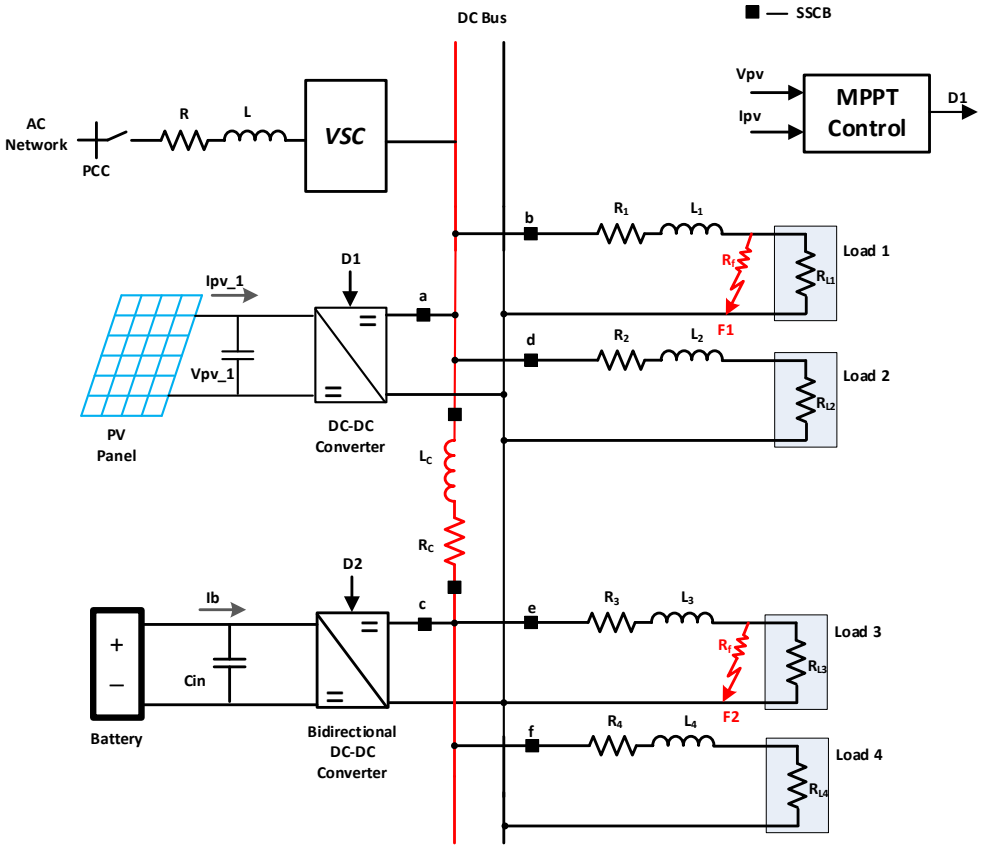

Fig. 2. Low Voltage DC Microgrid

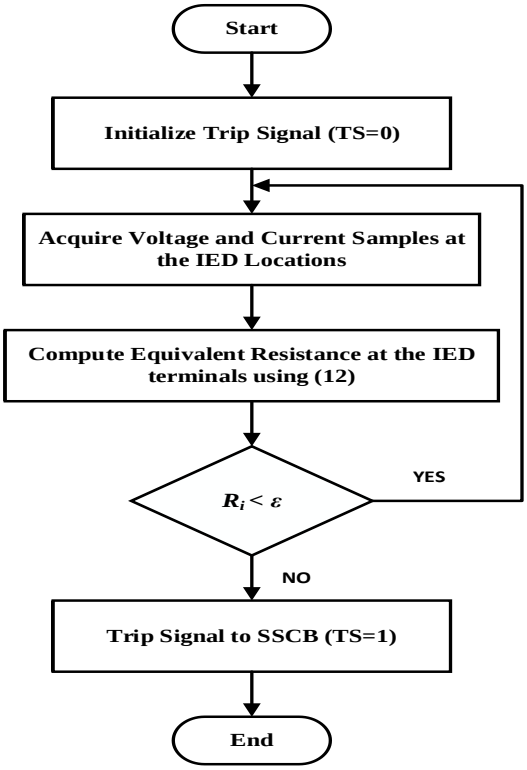

Fig. 3. The proposed protection method

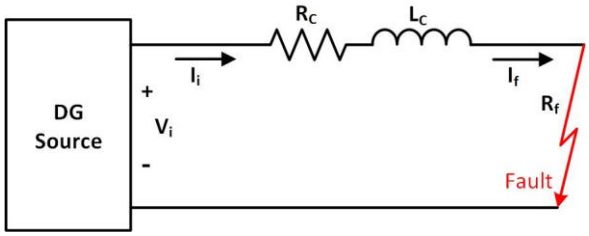

Fig. 4. Equivalent circuit of DG source during faulted condition

Table I

Components	Symbols	Value
DC Link Voltage	Vdc	50 V
Inductor	L1, L2	1mH
Capacitor	C1, C2, C3, C4	200 µF
Loads	Load (1, 2, 3, 4)	25 Ω each
Fault Resistance	R_f	0.1-1 Ω
Bi-directional Converter		200 W
DC-DC Boost Switching Frequency		5 kHz
Load Demand		100W
Battery Voltage		24 V
Battery Capacity		45 Ah
Cable Resistance	R1, R2, R3, R4 R_c	0.8 Ω/Km (0.5 Km) (1 Km)

V. SIMULATION RESULTS AND DISCUSSIONS

Solar Photovoltaic (SPV) based DGs are mostly used in residential and commercial places [26]. This paper incorporates SPV and battery systems in the microgrid network. The LVDC microgrid system shown in Figure 2 is used to demonstrate the proposed fault detection technique. DC microgrids are subjected to faults like the pole to ground fault, pole to pole fault, and DC arc faults[24]. Apart from this, two DC microgrid architectures, i.e., Unipolar and Bipolar DC bus system, exists in literature[25]. In this study, a unipolar isolated DC microgrid system is analyzed under the pole to ground faults. According to the simulation results, the proposed method for detecting faults is effective under various fault conditions.

In the first case, pole to ground fault (F_1) is conducted near load zone 1 at t =1.0 secs. The fault resistance R_f = 0.20 Ω. The voltage response at various DC buses is shown in Figure 5. It can be noticed that there is a sudden drop in the DC bus voltages after the fault. The extent of the voltage drop depends on the fault distance from the respective bus. The voltage drop at the fault location is high compared to other buses. Thus, the entire system gets affected. Figure 6 shows the behavior of fault current at various node points near the circuit breakers. The contribution of PV and battery current towards the fault can be seen in Figure 7. Figure 6 shows the magnitude of the fault current is less compared to

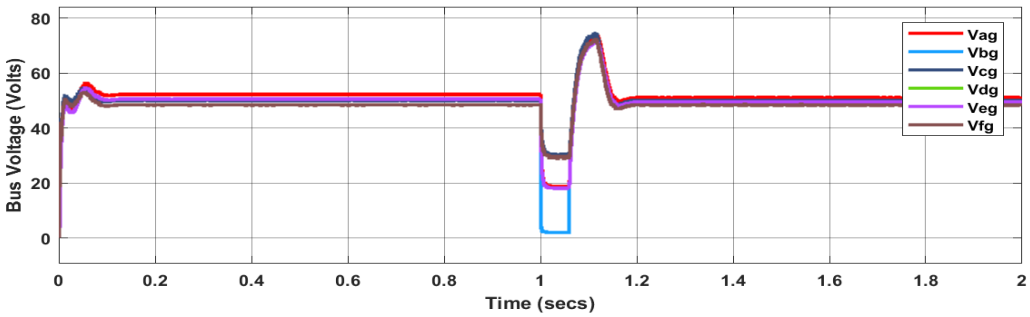

Fig. 5. DC Bus voltage for fault at location F_1 (t =1 to t = 1.08 secs)

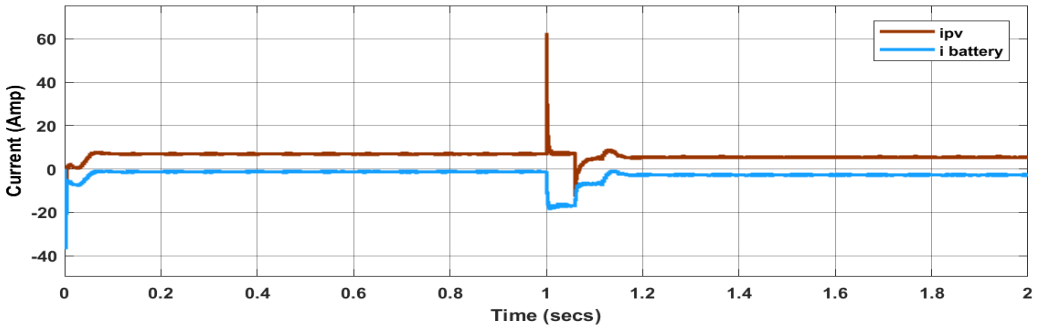

Fig. 6. Plot of source current during the fault F_1 (t =1 to t = 1.08 secs)

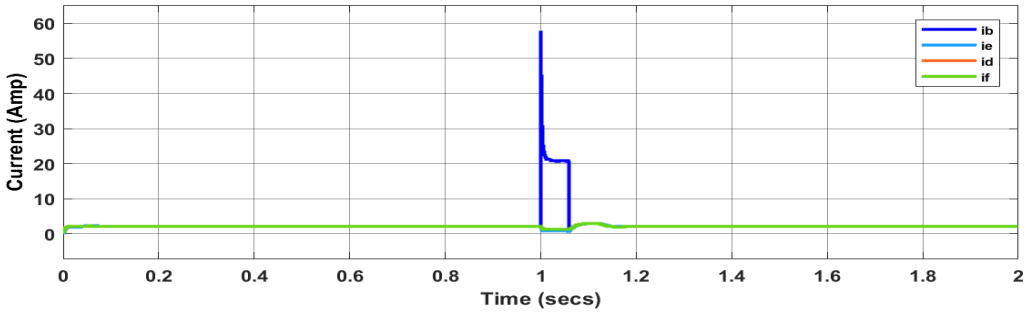

Fig. 7.Bus currents for the load zones (1, 2, 3, 4) during the fault F_1 (t =1 to t = 1.08 secs)

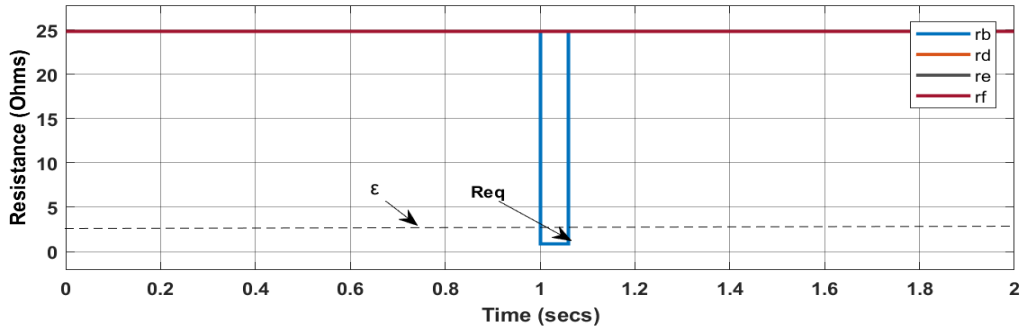

Fig. 8.Resistance seen at IEDs at the load zones (1,2,3,4) during the fault F_1 (t =1 to t = 1.08 secs)

any AC system faults. This shows that the power electronic converter limits the fault current. Figure 8 shows the resistance values seen by the IEDs present at various locations. It is evident that the equivalent resistance seen by the IED near load zone 1 is less compared to other zones. The trip signal will be sent to SSCB if the resistance value is less than the predefined threshold. Thus, the section having fault will be isolated. Figure 9 shows the bus voltages after the isolation of the faulty section. In the second case, a fault (F_2) near load zone 3 at the battery side is conducted. The

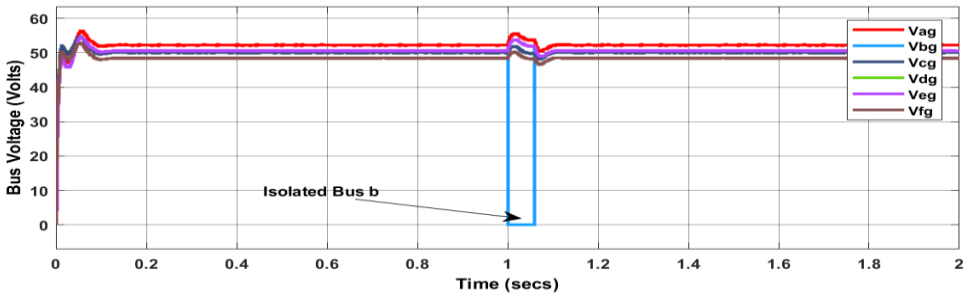

Fig. 9. Bus voltages after the isolation of fault by the SSCB

IED near the fault location of zone 3 sends the trip signal to the respective SSCB to disconnect that section.

Thus, it can be seen that after the isolation of the faulty section, the DC bus voltage of other buses is not affected except the faulted bus. So, the whole system is saved from de-energization. Therefore, fault identification and isolation, the dc microgrid does not need to be completely turned down. The results obtained validate that the presented fault detection approach is effective in detecting and isolating short circuit faults.

VI. CONCLUSION

In this paper, a local measurement-based fault detection technique is used to detect and isolate short circuit faults. The fault detection technique is demonstrated using an LVDC microgrid simulated in the MATLAB/Simulink environment. The method computes equivalent resistance measured at the terminals of IED to decide on sending the trip signal to SSCB. The proposed protection technique is used for detecting low impedance faults with varying fault resistance and fault location. The major advantage of this method is that it does not require any communication link. The voltage and current samples acquired locally at IED terminals are used for making decisions. The results obtained prove the efficacy of the presented fault detection methodology. The proposed method can be further extended for high impedance faults.

REFERENCES

[1] T. Dragičević, X. Lu, J.C. Vasquez, J.M. Guerrero, DC microgrids—Part II: A review of power architectures, applications, and standardization issues, IEEE Trans. Power Electron. 31 (2015) 3528–3549.

[2] L. Zhang, N. Tai, W. Huang, J. Liu, Y. Wang, A review on the protection of DC microgrids, J. Mod. Power Syst. Clean Energy. 6 (2018) 1113–1127.

[3] A.T. Elsayed, A.A. Mohamed, O.A. Mohammed, DC microgrids and distribution systems: An overview, Electr. Power Syst. Res. 119 (2015) 407–417.

[4] J.-D. Park, J. Candelaria, L. Ma, K. Dunn, DC ring-bus microgrid fault protection and identification of fault location, IEEE Trans. Power Deliv. 28 (2013) 2574–2584.

[5] S.D.A. Fletcher, P.J. Norman, K. Fong, S.J. Galloway, G.M. Burt, High-speed differential protection for smart DC distribution systems, IEEE Trans. Smart Grid. 5 (2014) 2610–2617.

[6] D. Salomonsson, L. Soder, A. Sannino, Protection of low-voltage DC microgrids, IEEE Trans. Power Deliv. 24 (2009) 1045–1053.

[7] M.E. Baran, N.R. Mahajan, Overcurrent protection on voltage-source-converter-based multiterminal DC distribution systems, IEEE Trans. Power Deliv. 22 (2006) 406–412.

[8] A. Meghwani, S.C. Srivastava, S. Chakrabarti, A new protection scheme for DC microgrid using current line derivative, in 2015 IEEE Power Energy Soc. Gen. Meet., IEEE, (2015) 1–5.

[9] T. Wang, A. Monti, Fault detection and isolation in DC microgrids based on singularity detection in the second derivative of local current measurement, IEEE J. Emerg. Sel. Top. Power Electron. (2020).

[10] A. Meghwani, S.C. Srivastava, S. Chakrabarti, A non-unit protection scheme for DC microgrid based on local measurements, IEEE Trans. Power Deliv. 32 (2016) 172–181.

[11] S. Dhar, R.K. Patnaik, P.K. Dash, Fault detection and location of photovoltaic based DC microgrid using differential protection strategy, IEEE Trans. Smart Grid. 9 (2017) 4303–4312.

[12] N. Bayati, H.R. Baghaee, A. Hajizadeh, M. Soltani, Localized protection of radial DC microgrids with high penetration of constant power loads, IEEE Syst. J. (2020).

[13] D. Jayamaha, N.W.A. Lidula, A.D. Rajapakse, Wavelet-based artificial neural networks for detection and classification of DC microgrid faults, in 2019 IEEE Power Energy Soc. Gen. Meet., IEEE, (2019) 1–5.

[14] Y.M. Yeap, N. Geddada, K. Satpathi, A. Ukil, Time-and frequency-domain fault detection in a VSC-interfaced experimental DC test system, IEEE Trans. Ind. Informatics. 14 (2018) 4353–4364.

[15] D.K.J.S. Jayamaha, N.W.A. Lidula, A.D. Rajapakse, Wavelet-Multi Resolution Analysis Based ANN Architecture for Fault Detection and Localization in DC Microgrids, IEEE Access. 7 (2019) 145371–145384. https://doi.org/10.1109/ACCESS.2019.2945397.

[16] A. Maqsood, D. Oslebo, K. Corzine, L. Parsa, Y. Ma, STFT cluster analysis for DC pulsed load monitoring and fault detection on naval shipboard power systems, IEEE Trans. Transp. Electrify. 6 (2020) 821–831.

[17] R. Mohanty, A.K. Pradhan, Protection of smart DC microgrid with ring configuration using parameter estimation approach, IEEE Trans. Smart Grid. 9 (2017) 6328–6337.

[18] R. Bhargav, B.R. Bhalja, C.P. Gupta, Novel fault detection and localization algorithm for low-voltage dc microgrid, IEEE Trans. Ind. Informatics. 16 (2019) 4498–4511.

[19] R. Mohanty, A.K. Pradhan, DC ring bus microgrid protection using the oscillation frequency and transient power, IEEE Syst. J. 13 (2018) 875–884.

[20] L. Kong, H. Nian, Fault Detection and Location Method for Mesh-Type DC Microgrid Using Pearson Correlation Coefficient, IEEE Trans. Power Deliv. 36 (2020) 1428–1439. https://doi.org/10.1109/tpwrd.2020.3008924.

[21] W. Congbo, J.I.A. Ke, Z. He, L.I. Zijin, L.I. Wei, L.I.U. Bohan, A Novel Protection Scheme for DC Distribution Network with Multi-terminal PV, in 2019 IEEE 2nd Int. Conf. Electron. Inf. Commun. Technol., IEEE, (2019) 857–861.

[22] M. Shamsoddini, B. Vahidi, R. Razani, H. Nafisi, Extending protection selectivity in low voltage DC microgrids using compensation gain and artificial line inductance, Electr. Power

Syst. Res. 188 (2020) 106530. https://doi.org/10.1016/j.epsr.2020.106530.

[23] R. Lazzari, L. Piegari, S. Grillo, M. Carminati, E. Ragaini, C. Bossi, E. Tironi, Selectivity and security of DC microgrid under line-to-ground fault, Electr. Power Syst. Res. 165 (2018) 238–249. https://doi.org/10.1016/j.epsr.2018.09.001.

[24] S. Dhar, P.K. Dash, Differential current-based fault protection with the adaptive threshold for multiple PV-based DC microgrid, IET Renew. Power Gener. 11 (2017) 778–790. https://doi.org/10.1049/iet-rpg.2016.0577.

[25] S. Ahmadi, I. Sadeghkhani, G. Shahgholian, B. Fani, J.M. Guerrero, Protection of LVDC Microgrids in Grid-Connected and Islanded Modes Using Bifurcation Theory, IEEE J. Emerg. Sel. Top. Power Electron. 9 (2019) 2597–2604. https://doi.org/10.1109/jestpe.2019.2961903.

[26] M.Kalarathi, K.Jayanthi. A Solar PV Fed Switched Capacitor Boost Circuit for DC Microgrid International Journal of Engineering Trends and Technology, (2021) 69(3),127-132.